Chemical Science

EDGE ARTICLE

View Article Online
View Journal | View Issue

Cite this: *Chem. Sci.*, 2019, **10**, 802

All publication charges for this article have been paid for by the Royal Society of Chemistry

Conformer-specific [1,2]*H*-tunnelling in captodatively-stabilized cyanohydroxycarbene (NC–C̈–OH)†

André K. Eckhardt, Frederik R. Erb and Peter R. Schreiner *

Received 20th August 2018
Accepted 31st October 2018

DOI: 10.1039/c8sc03720e

rsc.li/chemical-science

We report the gas-phase preparation of cyanohydroxycarbene by high-vacuum flash pyrolysis of ethyl 2-cyano-2-oxoacetate and subsequent trapping of the pyrolysate in an inert argon matrix at 3 K. After irradiation of the matrix with green light for a few seconds singlet *trans*-cyanohydroxycarbene rearranges to its *cis*-conformer. Prolonged irradiation leads to the formation of cyanoformaldehyde and isomeric isocyanoformaldehyde. *Cis*- and *trans*-cyanohydroxycarbene were characterized by matching matrix IR and UV/Vis spectroscopic data with *ab initio* coupled cluster and TD-DFT computations. *Trans*-cyanohydroxycarbene undergoes a conformer-specific [1,2]*H*-tunnelling reaction through a 33.3 kcal mol^{-1} barrier (the highest penetrated barrier of all H-tunnelling reactions observed to date) to cyanoformaldehyde with a half-life of 23.5 ± 0.5 d; this is the longest half-life reported for an H-tunnelling process to date. During the tunnelling reaction the *cis*-conformer remains unchanged over the same period of time and the Curtin–Hammett principle does not apply. NIR irradiation of the O–H stretching overtone does not enhance the tunnelling rate *via* vibrational activation. Push–pull stabilisation of hydroxycarbenes through σ- and π-withdrawing groups therefore is even more stabilizing than push–push substitution.

Introduction

Carbenes are reactive intermediates with a divalent carbon atom whose valence shell contains only six electrons, with triplet methylene (H–C̈–H) as its simplest representative.[1] In general, carbenes have a triplet electronic ground state according to Hund's rule but this can be affected through substitution.[1] Second-period substituents with lone pairs attached to the electron deficient carbene centre lead to singlet ground states. For example, cyanocarbene (**1**, H–C̈–CN) is an electronic ground state triplet molecule that can be photochemically interconverted by UV-light irradiation to its isomer isocyanocarbene (**2**, H–C̈–NC) with a singlet ground state as reported by Maier *et al.*[2] Further irradiation leads to cyclisation of **2** to singlet azacyclopropylidene (**3**) that can be photochemically re-opened to triplet **1** (Scheme 1); dicyanocarbene shows similar photochemical behaviour.[3]

Over the last decade we have prepared various singlet hydroxycarbenes (R–C̈–OH) and studied substituent effects on the experimentally observed [1,2]*H*-tunnelling reactions to the corresponding aldehydes at cryogenic temperatures, leading to the third reactivity paradigm of tunnelling control[4,5] next to thermodynamic and kinetic control of chemical reactions. The tunnelling half-life can be extended by introducing π-donors and completely be suppressed by introducing a second lone-pair carrying heteroatom substituent. Recently we demonstrated conformer-specific [1,2]*H*-tunnelling in trifluoromethylhydroxycarbene **4** (Scheme 1).[6] For the first time an energetically less favoured *cis*-conformer **4c** was photochemically produced from *trans*-conformer **4t**. While **4t** undergoes [1,2]*H*-tunnelling to trifluoroacetaldehyde **5**, **4c** remains unchanged over the same period of time. In contrast to parent hydroxymethylene **6** the tunnelling half-life of **4t** is extended from around 2 h in the parent system to 7 d due to the strong σ-electron-withdrawing –CF_3 group.

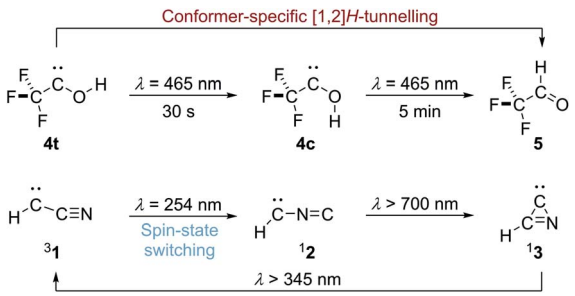

Scheme 1 Conformer-specific [1,2]*H*-tunnelling in singlet trifluoromethyl-hydroxycarbene (**4t**) and electronic spin-state switching in triplet cyanocarbene (^{3}**1**) to singlet isocyanocarbene (^{1}**2**) under UV light irradiation.

Institute of Organic Chemistry, Justus Liebig University, Heinrich-Buff-Ring 17, 35392 Giessen, Germany. E-mail: prs@uni-giessen.de

† Electronic supplementary information (ESI) available: Experimental procedures, detailed spectra and signal assignments, computational details coordinates, and absolute energies of all computed structures. See DOI: 10.1039/c8sc03720e

Our initial idea was to combine the reactivity of a cyano- and hydroxyl-group attached to a carbene centre in one molecule, namely hitherto unreported cyanohydroxycarbene (**7**), and study the photochemical isomerisation of the cyano group *vs.* [1,2]*H*-tunnelling of the hydroxyl group. The reactivity of singlet push–pull stabilized alkoxycyanocarbenes was already studied in cyclopropanation reactions.[7] The effect of a π-electron withdrawing substituent on [1,2]*H*-tunnelling in hydroxycarbenes has never been studied and is elaborated in the following. In radical chemistry the stabilisation of radicals by the combined action of an electron donating and electron withdrawing substituent is known as the captodative effect.[8] If this effect operates for **7**, it should also be stabilized and its tunnelling half-life extended relative to other hydroxycarbenes. Such findings would help in developing and sharpening concepts regarding the appearance of tunnelling and how it can be controlled through substitution.

Results and discussion

Our strategy for the preparation of **7** was high-vacuum flash pyrolysis (HVFP) of ethyl 2-cyano-2-oxoacetate (2-cyano-2-oxoacetic acid ethyl ester, **10**). Similar to our protocol for the gas-phase preparation of carbonic acid,[9] we used ester **10** for the preparation of 2-cyano-2-oxo acetic acid (**11**), an α-ketocarboxylic acid, which have proven to be suitable precursors for several hydroxycarbenes by thermal CO_2 extrusion (Scheme 2).[4] Ester **10** and its deuterated isotopologue were synthesized according to a literature procedure (see ESI† for details).[10] Pyrolysis of **10** at 900 °C and subsequent trapping of the pyrolysate at 3 K led to large amounts of CO_2 and ethylene (**12**) in the corresponding matrix isolation spectra, indicating nearly complete consumption of **10** and **11**, respectively, and confirms our suggested dissociation pathway (Scheme 2). Two conformers (*cis* and *trans*) of **11** were identified in the pyrolysis spectra as well; these can be readily interconverted by NIR irradiation (Fig. S28†).

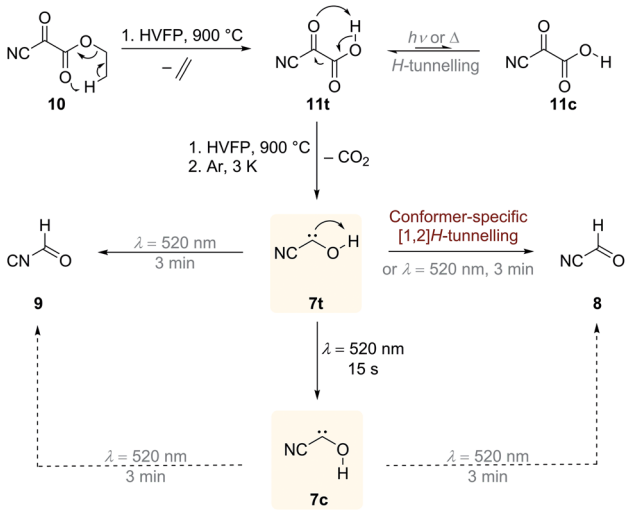

Scheme 2 Preparation of *cis*- and *trans*-cyanohydroxycarbene **7c** and **7t** by high-vacuum flash pyrolysis (HVFP) of ethyl 2-cyano-2-oxoacetate (**10**) at 900 °C. Pyrolysis of **10** first produces α-ketocarboxylic acid 2-cyano-2-oxo acetic acid (**11**), which further undergoes CO_2 extrusion to **7t** that is trapped in an argon matrix at 3 K. Carbene **7t** can be photochemically interconverted to its *cis*-conformer **7c**. After prolonged irradiation **7t** and **7c** rearrange to the thermodynamically preferred cyanoformaldehyde (**8**, formyl cyanide) and isocyanoformaldehyde (**9**, formyl isocyanide). Only *trans*-conformer **7t** slowly interconverts in a quantum mechanical conformer-specific [1,2]*H*-tunnelling reaction to **8**, while **7c** remains unchanged over the same period of time.

Further pyrolysis products were HCN, CO, **8**, and **9**, as identified by comparison with reference spectra;[11–14] **8** has recently been detected in interstellar media.[15] In addition, we also observed new unreported signals that we assign to **7t**. Irradiation of the matrix immediately after the pyrolysis with green light (λ = 520 nm) for three minutes led to complete disappearance of the signals of **7t** while, much to our surprise, the signals of both aldehydes, **8** and **9**, increased significantly (Fig. 1). With shorter irradiation times (5–30 s) the IR signals of **7t** were not completely depleted but new small signals appeared in the spectrum that we assign to *cis*-conformer **7c** (Fig. 1, red spectrum). Further irradiation led to the disappearance of these signals and again to an increase of **8** and **9**. An irradiation time of 15 s immediately after pyrolysis is sufficient for maximal conversion of **7t** to **7c**. Of course, aldehyde **8** is the [1,2]*H*-migration product of **7t**, while **9** might form from **8** at the cost of the excess energy after irradiation (*vide infra*).

The strongest bands of **7t** are located at 3511.8 and 1287.9 cm^{-1}, respectively. Furthermore, we also identified several weaker signals at 2156.8, 1343.8, 835.4, 829.8 and 821.6 cm^{-1} (Table S5†). The strongest signals of the *cis*-conformer **7c** are at 1272.2 and 801.9 cm^{-1}. Weaker signals are at 3365.4 cm^{-1} and 812.3 cm^{-1} (Table S6†). Our signal assignments of **7c** and **7t** are based on two IR difference spectra obtained from subtracting the spectra recorded after 15 s and 3 min irradiation of the matrix with a wavelength of 520 nm, respectively, from the spectrum recorded before irradiation of the same matrix in combination with *ab initio* AE-CCSD(T)/cc-pCVQZ coupled cluster anharmonic frequency computations. The signals of disappearing **7t** point downwards while the increasing signals of **7c**, **8**, and **9** point upwards (Fig. 1).

To confirm the formation of **7t** and **7c** we performed analogous experiments with **10** deuterated at the ethyl ester function (C_2D_4-**10′**) that produces deuterated **7′** in a very clean fashion because there is no exchange of acidic protons as is the case for α-ketocarboxylic acid precursors. The IR signal of the O–D stretching vibration of **7t′** and **7c′** are strongly affected by the isotopic substitution and were observed at 2598.1 cm^{-1} (exp. shift $\Delta\tilde{\nu}$ = 913.7 cm^{-1}, comp. anh. shift $\Delta\tilde{\nu}$ = 909.4 cm^{-1}) and 2498.7 cm^{-1} (exp. shift $\Delta\tilde{\nu}$ = 866.7 cm^{-1}, comp. anharm. shift $\Delta\tilde{\nu}$ = 826.7 cm^{-1}), respectively. The C–O–D in-plane and out-of-plane deformation vibrations of **7t′** are shifted to 1050.6 cm^{-1} (exp. shift $\Delta\tilde{\nu}$ = 293.2 cm^{-1}, comp. harm. shift $\Delta\tilde{\nu}$ = 301.3 cm^{-1}) and 642.4 cm^{-1} (exp. shift $\Delta\tilde{\nu}$ = 179.4 cm^{-1}, comp. harm. shift $\Delta\tilde{\nu}$ = 198.6 cm^{-1}) and for **7c′** to 1021.2 cm^{-1} (exp. shift $\Delta\tilde{\nu}$ = 56.6 cm^{-1}, comp. anh. shift $\Delta\tilde{\nu}$ = 42.4 cm^{-1}) and 649.0 cm^{-1} (exp. shift $\Delta\tilde{\nu}$ = 172.8 cm^{-1}, comp. harm. shift $\Delta\tilde{\nu}$ = 167.9 cm^{-1}), respectively. The remaining signals remain virtually unchanged

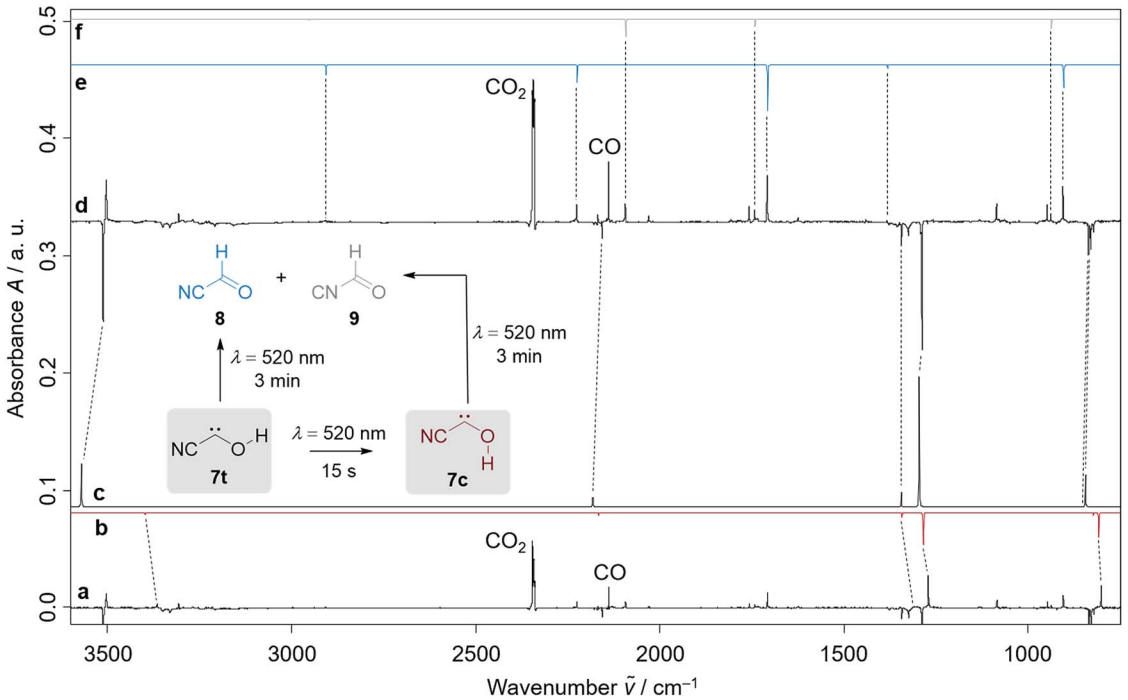

Fig. 1 (a): Experimental difference spectrum between the spectra recorded after 15 s irradiation of the matrix with a wavelength of 520 nm and the spectra immediately recorded after 4 h pyrolysis of ethyl 2-cyano-2-oxoacetate (**10**) at 900 °C; (b and c): computed anharmonic AE-CCSD(T)/cc-pCVQZ vibrational spectra (unscaled) of *cis*-cyanohydroxycarbene (**7c**, red, b) and *trans*-cyanohydroxycarbene (**7t**, black, c); (d): experimental difference spectrum between the spectra recorded after 3 min irradiation of the matrix with a wavelength of 520 nm and the spectra immediately recorded after 4 h pyrolysis of ethyl 2-cyano-2-oxoacetate (**10**) at 900 °C; (e and f): experimentally observed vibrational frequencies of isocyanoformaldehyde (**9**, grey, f) and cyanoformaldehyde (**8**, blue, e) in combination with computed AE-CCSD(T)/cc-pCVQZ anharmonic intensities.

(Fig. S27†). A complete band assignment is summarized in the ESI (Tables S7 and S8†).

We also proved the formation of **7t** using UV/Vis spectroscopy because we experimentally observed a HOMO – LUMO transition at λ_{max} = 467 nm that is typical for hydroxycarbenes[5,16,17] in this range (Fig. 2 and S30†). We computed the electronic transitions with time dependent density functional theory at TD-B3LYP/6-311++G(2d,2p) to be at 531.0 nm with an oscillator strength of $f = 0.0045$ for **7t**, in good agreement with experiment. For **7c** the HOMO – LUMO transition is computed at 535.5 nm ($f = 0.0054$). However, we were not able to record a specific UV/Vis spectrum for **7c** (see red spectrum after 15 s 520 nm irradiation in Fig. 2) with shorter irradiation times. The similarity of the computed absorptions of **7t** and **7c** helps us rationalize why both conformers are completely depleted upon prolonged irradiation (blue, orange and grey spectrum in Fig. 2). We assigned the slightly increasing signals at around 300–370 nm to **8** and **9** according to our observations in the IR spectra and through comparison with the literature and computations (Table S3 and S4†).[11]

In the dark the IR signals of **7t** disappear with a half-life of around $\tau = 23.5 \pm 0.5$ d (temperature independent in the 3–12 K interval) through a quantum mechanical tunnelling (QMT) process as observed for several other hydroxycarbenes.[4] The disappearance of the signal of **7t** at around 1288 cm^{-1} over a time range of 47 days is shown in Fig. 3. In contrast to the

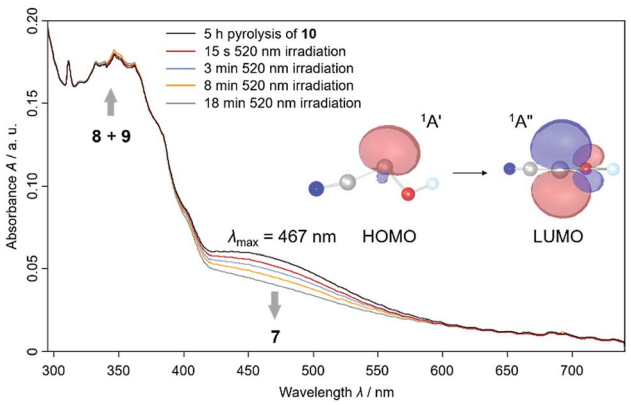

Fig. 2 Experimental UV/Vis spectra of the pyrolysate of 2-cyano-2-oxo-acetic acid ethyl ester (**10**) including cyanohydroxycarbene (**7**) in argon at 8 K. After 5 h pyrolysis of **10** at 900 °C the black spectrum was recorded. The broad signal of *trans*-cyanohydroxycarbene (**7t**) between 400 and 550 nm disappears after prolonged irradiation with a wavelength of 520 nm of the same matrix. We assigned the slightly increasing signals around 350 nm to the photoproducts of **7t**, namely cyanoformaldehyde (**8**) and isocyanoformaldehyde (**9**). The NBOs for the electronic transition of **7t** were computed at the HF/6-311++G(2d,2p) level of theory based on the AE-CCSD(T)/cc-pCVQZ optimized geometry of **7t**. HOMO = highest occupied molecular orbital; LUMO = lowest unoccupied molecular orbital; NBO = natural bond orbital.

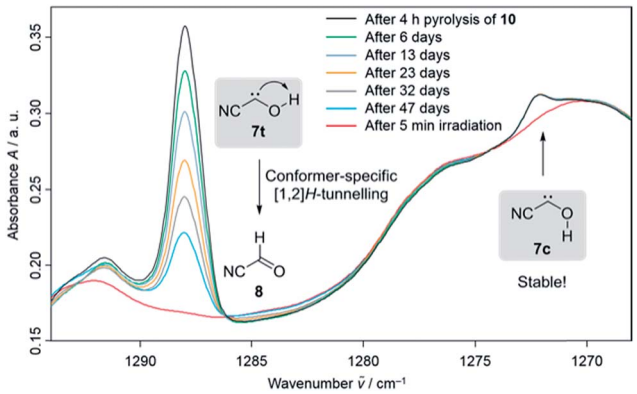

Fig. 3 Conformer-specific [1,2]*H*-tunnelling of *trans*-cyanohydroxycarbene (**7t**) with a tunnelling half-life of $\tau = 23.5 \pm 0.5$ d over a time period of 47 days monitored by the signal decay at around 1288 cm^{-1}. The amount of the *cis*-conformer **7c** remained unchanged over the same period of time at around 1272 cm^{-1} (marked with an arrow). After 5 min irradiation of the matrix with a wavelength of 520 nm both carbene signals are completely depleted (red spectrum).

photochemical interconversion of **7t** to **8** and **9**, only **8** forms through [1,2]*H*-tunnelling. Hence, the excess energy after tunnelling through the barrier is efficiently distributed through intramolecular vibrational relaxation (IVR) and removed by the cryogenic surroundings.

There is not enough excess energy left for subsequent isomerisation of **8** to **9** as in the photochemical interconversion (for details of the potential energy surface, see Fig. 4). The small signal of **7c** at around 1272 cm^{-1} remained unchanged over the same period of time (Fig. 3). Hence, only the *trans*-conformer **7t** undergoes [1,2]*H*-tunnelling. To the best of our knowledge this is only the second example of a conformer-specific *H*-tunnelling reaction (which was first observed for **4t**).[6] As for all other hydroxycarbenes, deuteration of the hydroxyl group suppresses tunnelling completely due to the higher mass. After two weeks in the dark, the matrix spectra with isolated O–D **7t′** were completely unchanged.

We also attempted to stimulate [1,2]*H*-tunnelling in **7t** through vibrationally activated tunnelling (VAT)[18,19] (the [1,2]*H*-tunnelling half-life from an excited vibrational mode is computed to be around 2 h (Table S13†)) by near infrared (NIR) laser irradiation of the measured O–H stretching vibration overtone of **7t** at 6840.2 cm^{-1} (1461.95 nm ≙ 19.6 kcal mol^{-1}) (Fig. 4 and S21†). However, the spectrum remained unchanged after 2 h irradiation. We did not even observe an enrichment of the energetic less favoured **7c** isomer because we irradiated with a photon energy less than the computed torsional barrier for *trans–cis* isomerisation (25.7 kcal mol^{-1}; see PES in Fig. 4). Hence, excitation of the O–H stretching overtone is ineffective for VAT in hydroxycarbenes and the excitation of the C–O–H deformation vibration seems much more effective from a theoretical point of view because this vibration or "reactive mode" pushes the system towards the tunnelling product **8**. Unfortunately, the signal for this specific overtone could not be detected experimentally due to its very low intensity. Also, IVR is likely to be much too fast (ps timescale[20]) and too inefficient for the excitation of the overtone of the C–O–H deformation vibrational mode ($v = 2$). Furthermore, the torsional barrier for *trans–cis* isomerisation in **7** is one of the highest known barriers for intramolecular OH torsion in comparison to familiar acids,[21,22] alcohols[23] or hydroxycarbenes.[6]

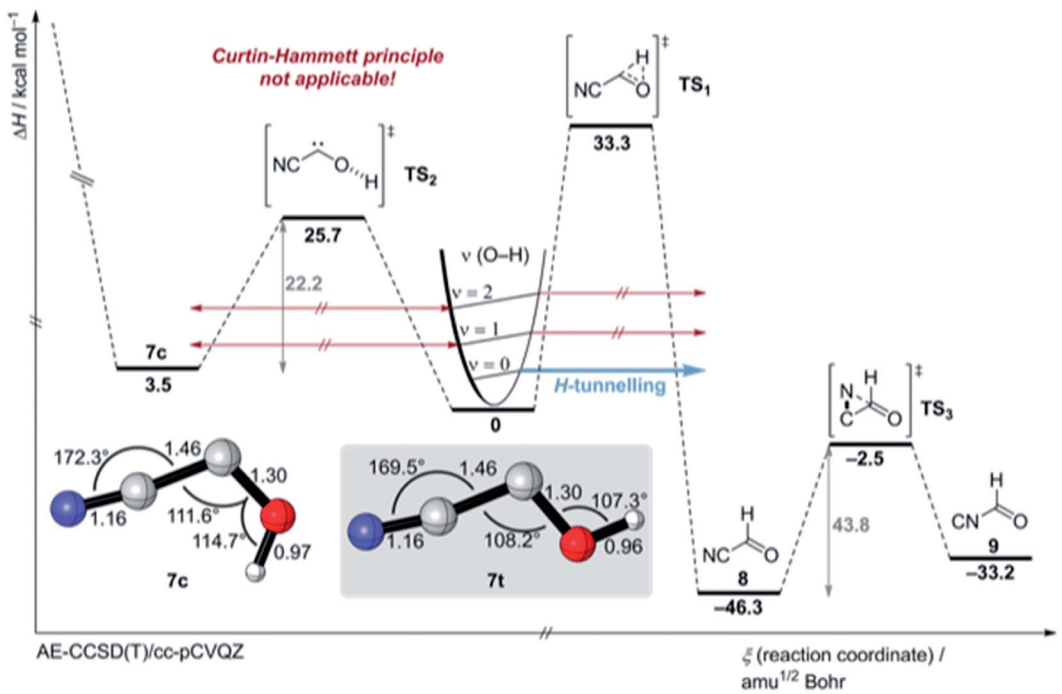

Fig. 4 Potential energy surface around cyanohydroxycarbene (**7**) (colour code: carbon: grey, nitrogen: blue, oxygen: red, hydrogen: white) at the AE-CCSD(T)/cc-pCVQZ + ZPVE level of theory. For an extended version of the PES see Fig. S45 and S46.†

We computed the most important part of the potential energy surface (PES) around **7** at the AE-CCSD(T)/cc-pVCQZ and an extended PES version at the B3LYP/6-311++G(2d,2p) + harmonic zero-point vibrational energies (ZPVE) level of theory (Fig. 4, S45 and S46†). *Cis*- and *trans*-**7** are planar C_s symmetric molecules that have closed-shell singlet $^1A'$ electronic ground states. There is only one C_1 point group triplet state isomer ^{3}**7** at AE-CCSD(T)/cc-pVCQZ that is much higher in energy (T_0 = 20.4 kcal mol^{-1}). The singlet triplet gap in **7t** is the smallest in comparison to all other prepared hydroxycarbenes, in which the triplet state typically lies around 25 kcal mol^{-1} higher in energy than the singlet electronic ground state. The C–O bond length of **7t** and **7c** of 1.30 Å is much shorter than a typical C–O bond (*e.g.*, 1.41 Å in methanol[23]) due to π-type stabilisation of the electron-deficient carbene centre through the oxygen p lone pair (Fig. S37 and S41†). A Wiberg bond index of approximately 1.22 is computed for the C–O-bond in **7t** and **7c**, indicative of zwitterionic and polarized allene-type resonance structures (Fig. S43 and S44†).[1] A natural resonance theory (NRT) analysis highly favours the zwitterionic resonance structures over the neutral and allenic species (Fig. S43 and S44†).

In contrast to **4**, in which both conformers are almost equal in energy, **7t** and **7c** differ by 3.5 kcal mol^{-1}. The reaction barrier for the observed conformer-specific [1,2]*H*-tunnelling reaction of **7t** to **8** is 33.3 kcal mol^{-1} (**TS$_1$**, C_s) and therefore 2.6 kcal mol^{-1} higher than in the tunnelling reaction of **4t** (Fig. 5). Both conformers of **7** are connected by a 25.7 kcal mol^{-1} high C_1 transition state **TS$_2$** in the forward (**7t** → **7c**) and 22.2 kcal mol^{-1} in the reverse (**7c** → **7t**) reaction. Hence, interconversion and pre-equilibration of **7t** to **8** is not given at cryogenic temperatures and the Curtin–Hammett principle is not applicable.[6] We did not locate a transition state directly connecting **7c** and **8** or **9**, respectively.

Aldehyde **8** is favoured by 13.1 kcal mol^{-1} over **9**; both isomers are connected by a C_1 transition structure **TS$_3$** with a 43.8 kcal mol^{-1} barrier in the forward (**8** → **9**) and a 30.7 kcal mol^{-1} barrier in the reverse (**9** → **8**) direction. Both isomers can be interconverted photochemically; a tunnelling

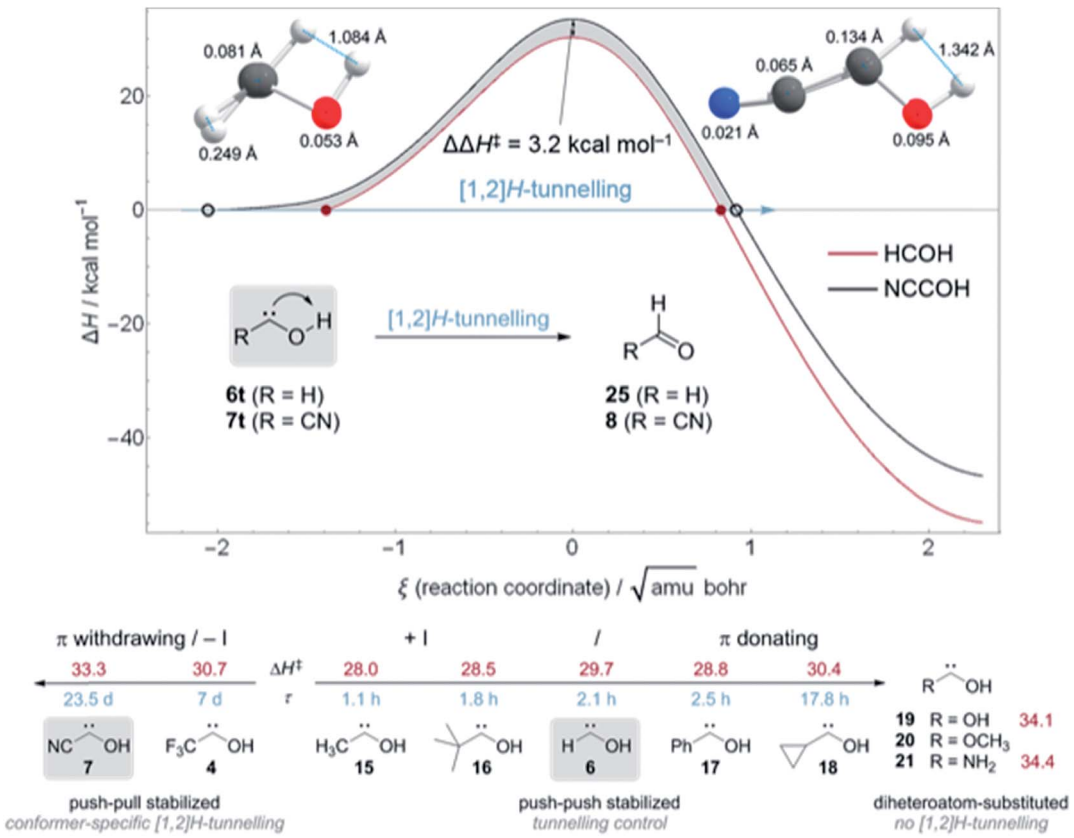

Fig. 5 Top: Comparison of the computed ZPVE-corrected reaction barriers for [1,2]*H*-tunnelling in hydroxymethylene (**6t**, red) and cyanohydroxycarbene (**7t**, black) at B3LYP/cc-pVTZ. The barrier for **7t** is 3.2 kcal mol^{-1} higher and much wider than in parent hydroxymethylene; the difference between the two barriers is depicted by the grey area between the two reaction profiles. The two structures on the top (colour code: carbon, grey; oxygen, red; hydrogen, white) show the atomic motions along the reaction coordinate between the two turning points (depicted as red disks and black circles) at the zero-energy level. Bottom: Matrix-isolated hydroxycarbenes, their experimentally determined tunnelling half-lives τ and computed tunnelling barriers for the [1,2]*H*-shift to the corresponding aldehydes $\Delta H^{\ddagger}$ (in kcal mol^{-1}) at the coupled cluster level of theory with at least a triple-ζ basis set. Push–pull stabilized hydroxycarbenes show conformer-specific [1,2]*H*-tunnelling while for most of the push–push stabilized hydroxycarbenes (**15**, **16**, and **18**) the third reactivity paradigm tunnelling control is applicable. Second-period diheteroatom–substituted hydroxycarbenes do not show [1,2]*H*-tunnelling although the reaction barriers are only slightly higher than those of cyanohydroxycarbene (**7**).

isomerisation reaction was experimentally not observed due to the very high and broad reaction barrier and the involvement of heavy atom movement along the reaction path that makes tunnelling less likely.[11,24] The transition states ($\mathbf{TS_5}$ and $\mathbf{TS_{10}}$) for the isomerisation of the nitrile group in **7** (not shown here, for an extended version of the PES see Fig. S45 and S46†) are computed to 44.9 and 48.1 kcal mol^{-1}, respectively, and these are in the same energetic region as transition state $\mathbf{TS_4}$ for the dissociation of **7c** into HCN and CO (46.1 kcal mol^{-1}).

We computed the tunnelling half-life of **7t** with the semi-classical one-dimensional Wentzel–Kramers–Brillouin (WKB) tunnelling model[25–27] at the AE-CCSD(T)/cc-pCVQZ//MP2/cc-pVTZ level of theory to τ = 77 d, in good agreement with the experimental result (see ESI† for details). For deuterated **7t′** the tunnelling half-life is computed to several thousand years. We also carried out multidimensional instanton[28] and canonical variational transition state theory in combination with small curvature tunnelling correction (CVT/SCT)[29,30] computations at B3LYP/cc-pVTZ, which describes the PES around **7** almost as well as the high level coupled cluster computations (see ESI† for further details). With the instanton approach the tunnelling half-life is determined to $\tau \approx$ 40 d in an almost perfect agreement with experiment (Table S12†).[31] To the best of our knowledge, the experimentally observed *H*-tunnelling process here passes through the highest reaction barrier (33.3 kcal mol^{-1}) resulting in the longest hitherto observed *H*-tunnelling half-life (23.5 ± 0.5 d) reported to date.[32]

We computed the ZPVE-corrected reaction barriers for [1,2]*H*-tunnelling in **6t** to formaldehyde (**25**) and **7t** to **8** at B3LYP/cc-pVTZ (Fig. 5, Top) and compared the different barrier shapes with each other. The barrier for the isomerisation of **7t** is 3.2 kcal mol^{-1} higher in energy and the overall reaction almost 8 kcal mol^{-1} less exothermic than in **6t** → **25**, resulting in a much wider barrier according to the Bell–Evans–Polanyi principle. The difference between the two reaction profiles is depicted as the grey area in Fig. 5. Tunnelling through this area increases the half-life of **7t** to almost 24 d in contrast to 2.1 h in **6t**. Due to the much wider barrier the tunnelling distances of every atom along the reaction coordinate change. We compared the atomic motion along the reaction arc of **6t** and **7t** between the two classical turning points (depicted as red disks and black circles in Fig. 5 (Top)) at the zero-energy level that already includes the attempt energy for tunnelling because the reaction barriers are fully ZPVE corrected in which the reactive mode is already included. Note that the distances of atom movement along the reaction arc slightly differ from the Euclidean distance of the two turning point geometries because the reaction coordinate is multidimensional. The two structures on the top in Fig. 5 clearly show that every atom participates in the tunnelling process and not only the transferred hydrogen, which, of course, contributes the most.[31,33] Due to the smaller barrier width for the isomerisation of **6t** the transferred hydrogen only moves 1.084 Å in contrast to the 1.342 Å in **7t**. The tunnelling distances of the heavier oxygen and carbene carbon atom are almost doubled in **7t** in comparison to **6t**.

Fig. 5 (Bottom) summarizes the QMT reactivity of hydroxycarbenes prepared to date. Additional π-donors (+M) increase the tunnelling half-life of parent **6**[16] from 2.1 h to 2.5 h in phenylhydroxycarbene[17] (**17**) and almost 18 h in cyclopropylhydroxycarbene[34] (**18**) through push–push stabilisation.[1] With an inductive donating (+I) substituent, like a methyl group in methylhydroxycarbene[5,33] **15** or *tert*-butyl group in *tert*-butylhydroxycarbene[35] **16** the tunnelling half-lives slightly decrease to 1.1 and 1.8 h, respectively, in comparison to **6**. However, the second substituent in **15**, **16**, and **18** leads to the appearance of tunnelling control in which the product through the higher but narrower barrier forms, irrespective of the kinetic preference.[4,5,34,35] [1,2]*H*-tunnelling is completely suppressed in diheteroatom-substituted hydroxycarbenes dihydroxycarbene[36] (**19**), methoxyhydroxycarbene[36] (**20**), and aminohydroxycarbene (**21**).[4] Even in the simplest aminocarbene, aminomethylene, [1,2]*H*-tunnelling was not observed due to the strong π-donation of the nitrogen atom.[37]

On the other hand, electron-withdrawing groups seem to stabilize hydroxycarbenes even more than non-heteroatom electron donating substituents through push–pull stabilisation (Fig. 5, bottom left).[1] The tunnelling half-life with an inductive electron withdrawing (−I) CF_3-group in **4** is 7 d and therefore almost 80 times larger than in parent **6**. In this study we determined the tunnelling half-life of **7** with a π withdrawing cyano group to 23.5 ± 0.5 d, *i.e.*, 269 times larger than in **6**.

Hence, π-withdrawing groups (−M) seem to have a stronger effect on the tunnelling half-lives than −I substituents. Even the energetically less favourable *cis*-conformer **4c** and **7c** were experimentally observed, likely due to push–pull stabilisation of the electron deficient carbene centre. These findings led to the notion of conformer-specific [1,2]*H*-tunnelling[6] for which we presented a second example here.

Conclusions

We present the first spectroscopic characterisation of cyanohydroxycarbene by matrix isolation IR and UV/Vis spectroscopy. The energetically less preferred *cis*-conformer can be photochemically generated from the *trans* conformer. The *trans*-conformer undergoes conformer specific [1,2]*H*-tunnelling from the vibrational ground state to cyanoformaldehyde through a 33.3 kcal mol^{-1} high but narrow barrier with a half-life of 23.5 ± 0.5 d (computed 40–80 d) while the *cis*-conformer remains virtually unchanged over the same period of time. Based on our experimental results and *ab initio* AE-CCSD(T)/cc-pCVQZ computations, both conformers are C_s symmetric singlet ground state carbenes that are connected by a high rotational barrier (25 kcal mol^{-1}) so that interconversion at cryogenic temperatures is suppressed and the Curtin–Hammett principle is not applicable. Both carbene conformers can be photochemically isomerised through prolonged irradiation to cyanoformaldehyde and isocyanoformaldehyde. Vibrationally activated tunnelling by means of near infrared excitation of the O–H stretching overtone of *trans*-cyanohydroxycarbene and photochemical isomerisation of cyanohydroxycarbene to isocyanohydroxycarbene was experimentally not observed.

In general, hydroxycarbenes can be stabilized through electron donating and withdrawing substituents. Hereby, the

half-lives slightly increase through π-donating groups (push–push stabilisation) and significantly extend through σ-donation (+I) and, as demonstrated here, even better through π-withdrawing groups (push–pull stabilisation, captodative effect). Tunnelling is completely suppressed through a strong second π-donating substituent such as heteroatoms bearing lone pairs.

Conflicts of interest

There are no conflicts to declare.

Acknowledgements

A. K. E. thanks the Fonds der Chemischen Industrie for a scholarship. The authors thank Dr Dennis Gerbig and Henrik Quanz (both JLU Giessen) for setting up the NIR-Laser.

Notes and references

1 D. Bourissou, O. Guerret, F. P. Gabbaï and G. Bertrand, *Chem. Rev.*, 2000, **100**, 39–92.
2 G. Maier, H. P. Reisenauer and K. Rademacher, *Chem.–Eur. J.*, 1998, **4**, 1957–1963.
3 G. Maier, H. P. Reisenauer and R. Ruppel, *Eur. J. Org. Chem.*, 2003, **2003**, 2695–2701.
4 P. R. Schreiner, *J. Am. Chem. Soc.*, 2017, **139**, 15276–15283.
5 P. R. Schreiner, H. P. Reisenauer, D. Ley, D. Gerbig, C. H. Wu and W. D. Allen, *Science*, 2011, **332**, 1300–1303.
6 A. Mardyukov, H. Quanz and P. R. Schreiner, *Nat. Chem.*, 2017, **9**, 71–76.
7 R. A. Moss, T. Zdrojewski, K. Krogh-Jespersen, M. Włostowski and A. Matro, *Tetrahedron Lett.*, 1991, **32**, 1925–1928.
8 H. G. Viehe, Z. Janousek, R. Merenyi and L. Stella, *Acc. Chem. Res.*, 1985, **18**, 148–154.
9 H. P. Reisenauer, J. P. Wagner and P. R. Schreiner, *Angew. Chem., Int. Ed.*, 2014, **53**, 11766–11771.
10 O. Achmatowicz and J. Szymoniak, *Tetrahedron*, 1982, **38**, 1299–1302.
11 K. Banert, J. R. Fotsing, M. Hagedorn, H. P. Reisenauer and G. Maier, *Tetrahedron*, 2008, **64**, 5645–5648.
12 D. J. Clouthier and D. Moule, *J. Am. Chem. Soc.*, 1987, **109**, 6259–6261.
13 W. Lewis-Bevan, R. D. Gaston, J. Tyrrell, W. D. Stork and G. L. Salmon, *J. Am. Chem. Soc.*, 1992, **114**, 1933–1938.
14 M. Gronowski, P. Eluszkiewicz and T. Custer, *J. Phys. Chem. A*, 2017, **121**, 3263–3273.
15 J. R. Anthony, J. M. Hollis, F. J. Lovas, D. S. Wilmer, P. R. Jewell and D. S. Meier, *Astrophys. J., Lett.*, 2008, **675**, L85.
16 P. R. Schreiner, H. P. Reisenauer, F. C. Pickard IV, A. C. Simmonett, W. D. Allen, E. Matyus and A. G. Csaszar, *Nature*, 2008, **453**, 906–909.
17 D. Gerbig, H. P. Reisenauer, C. H. Wu, D. Ley, W. D. Allen and P. R. Schreiner, *J. Am. Chem. Soc.*, 2010, **132**, 7273–7275.
18 M. Pettersson, E. M. S. Maçôas, L. Khriachtchev, R. Fausto and M. Räsänen, *J. Am. Chem. Soc.*, 2003, **125**, 4058–4059.
19 E. M. Greer, K. Kwon, A. Greer and C. Doubleday, *Tetrahedron*, 2016, **72**, 7357–7373.
20 S. Perry David, G. A. Bethardy and X. Wang, *Ber. Bunsen-Ges. Phys. Chem.*, 1995, **99**, 530–535.
21 M. Pettersson, E. M. S. Maçôas, L. Khriachtchev, J. Lundell, R. Fausto and M. Räsänen, *J. Chem. Phys.*, 2002, **117**, 9095–9098.
22 E. M. S. Maçôas, L. Khriachtchev, M. Pettersson, R. Fausto and M. Räsänen, *J. Am. Chem. Soc.*, 2003, **125**, 16188–16189.
23 F. H. Allen, O. Kennard, D. G. Watson, L. Brammer, A. G. Orpen and R. Taylor, *J. Chem. Soc., Perkin Trans. 2*, 1987, **0**, S1–S19.
24 W. T. Borden, *WIREs Comput. Mol. Sci.*, 2016, **6**, 20–46.
25 G. Wentzel, *Z. Phys.*, 1926, **38**, 518–529.
26 H. A. Kramers, *Z. Phys.*, 1926, **39**, 828–840.
27 L. Brillouin, *C. R. Acad. Sci.*, 1926, **183**, 24–26.
28 J. B. Rommel, T. P. M. Goumans and J. Kästner, *J. Chem. Theory Comput.*, 2011, **7**, 690–698.
29 A. Kuppermann and D. G. Truhlar, *J. Am. Chem. Soc.*, 1971, **93**, 1840–1851.
30 R. T. Skodje, D. G. Truhlar and B. C. Garrett, *J. Phys. Chem.*, 1981, **85**, 3019–3023.
31 J. Kästner, *Chem.–Eur. J.*, 2013, **19**, 8207–8212.
32 H. Rostkowska, L. Lapinski and M. J. Nowak, *Phys. Chem. Chem. Phys.*, 2018, **20**, 13994–14002.
33 A. K. Eckhardt, D. Gerbig and P. R. Schreiner, *J. Phys. Chem. A*, 2018, **122**, 1488–1495.
34 D. Ley, D. Gerbig, J. P. Wagner, H. P. Reisenauer and P. R. Schreiner, *J. Am. Chem. Soc.*, 2011, **133**, 13614–13621.
35 D. Ley, D. Gerbig and P. R. Schreiner, *Chem. Sci.*, 2013, **4**, 677–684.
36 P. R. Schreiner and H. P. Reisenauer, *Angew. Chem., Int. Ed.*, 2008, **47**, 7071–7074.
37 A. K. Eckhardt and P. R. Schreiner, *Angew. Chem., Int. Ed.*, 2018, **57**, 5248–5252.

